

migS, a *cis*-acting site that affects bipolar positioning of *oriC* on the *Escherichia coli* chromosome

Yoshiharu Yamaichi^{1,2} and Hironori Niki^{1,*}

¹Radioisotope Center, National Institute of Genetics, Yata 1111, Mishima 411-8540 Japan and ²Graduate School of Medicine, Kumamoto University, Kuhonji 4-24-1, Kumamoto 862-0976, Japan

During replication of the *Escherichia coli* chromosome, the replicated Ori domains migrate towards opposite cell poles, suggesting that a *cis*-acting site for bipolar migration is located in this region. To identify this *cis*-acting site, a series of mutants was constructed by splitting subchromosomes from the original chromosome. One mutant, containing a 720 kb subchromosome, was found to be defective in the bipolar positioning of *oriC*. The creation of deletion mutants allowed the identification of *migS*, a 25 bp sequence, as the *cis*-acting site for the bipolar positioning of *oriC*. When *migS* was located at the replication terminus, the chromosomal segment showed bipolar positioning. *migS* was able to rescue bipolar migration of plasmid DNA containing a mutation in the SopABC partitioning system. Interestingly, multiple copies of the *migS* sequence on a plasmid in *trans* inhibited the bipolar positioning of *oriC*. Taken together, these findings indicate that *migS* plays a crucial role in the bipolar positioning of *oriC*. In addition, real-time analysis of the dynamic morphological changes of nucleoids in wild-type and *migS* mutants suggests that bipolar positioning of the replicated *oriC* contributes to nucleoid organization.

The EMBO Journal (2004) 23, 221–233. doi:10.1038/sj.emboj.7600028; Published online 18 December 2003

Subject Categories: genome stability & dynamics; microbiology & pathogens

Keywords: bacteria; migration; mukB; nucleoids; partitioning; segregation

Introduction

The replicon theory of bacterial chromosome segregation suggested that newly replicated chromosomes were segregated into their daughter cells through a passive, membrane-bound process (Jacob *et al.*, 1963). In recent years, it has become clear that bacterial chromosome segregation is, in fact, an active process involving specific mechanisms (reviewed in Gordon and Wright, 2000; Hiraga, 2000; Draper and Gober, 2002); however, some basic questions still remain to be resolved. One of these questions is whether a *cis*-acting centromere-like site exists in the bacterial genome. In prokar-

yotes, a centromere-like structure is considered to be a *cis*-acting DNA sequence involved in chromosome migration, as opposed to a site for attachment to microtubules in eukaryotes. Cytological experiments using fluorescence probes have revealed that replicated *oriC* segments abruptly migrate towards opposite poles in several bacteria (Glaser *et al.*, 1997; Gordon *et al.*, 1997; Lewis and Errington, 1997; Webb *et al.*, 1997; Niki and Hiraga, 1998; Jensen and Shapiro, 1999). In replicating *Escherichia coli* cells, bipolar migration involves not only the *oriC* segment but also the large flanking region, the Ori domain, which is about 900 kb of the chromosomal segment including *oriC* (Niki *et al.*, 2000). If a *cis*-acting site is involved in bipolar migration, it is expected to be located within this large chromosomal region. Clearly, the *oriC* sequence itself is not sufficient for bipolar migration of *oriC* on the chromosome because an *oriC* plasmid is localized randomly in the cytosolic region (Niki and Hiraga, 1999) and bipolar migration is not affected in a mutant lacking *oriC* (Gordon *et al.*, 2002). Previous studies have suggested the presence of a *cis*-acting centromere-like site in prokaryotes. In *Bacillus subtilis*, a 150 kb chromosomal segment to the left of *oriC* was found to be necessary for attachment to the end-pole during ongoing sporulation (Wu and Errington, 2002). Chromosomal attachment to the end pole position in *B. subtilis* is mediated by the Rac protein, which forms a bridge between chromosomal sites and division protein DivIVA that is located at the end pole (Edwards and Errington, 1997; Ben-Yehuda *et al.*, 2003).

Extrachromosomal elements in bacteria have their own partitioning mechanisms, including a *cis*-acting site or a centromere-like element (Gordon and Wright, 2000; Hiraga, 2000; Draper and Gober, 2002). The partitioning mechanisms of sex factor F and prophage P1 have been actively investigated. In both extrachromosomal elements, three components which consist of two proteins and a *cis*-acting DNA site are involved in accurate segregation: *sopA*, *sopB*, and *sopC* in F plasmid, and *parA*, *parB*, and *parS* in P1 prophage. Homologies in amino acid sequences between SopA and ParA, and SopB and ParB have been identified, and these proteins function in a similar manner in plasmid partitioning (Davis and Austin, 1988; Funnell, 1988; Mori *et al.*, 1989; Watanabe *et al.*, 1992). In the case of the *sopABC* partitioning system, the SopB protein binds to the *sopC* DNA site, and SopA interacts with the SopB–*sopC* complex so that plasmid DNAs with *sopC* can faithfully segregate towards daughter cells. The plasmid DNAs are localized at the midcell, and the daughter plasmids migrate to the 1/4 and 3/4 positions of the cell length during the cell division cycle (Gordon *et al.*, 1997; Niki and Hiraga, 1997). In addition to extrachromosomal elements, homologs of the *sopA* and *sopB* genes (the ParA and ParB families) have been found in at least 77 various bacterial chromosomes, including *B. subtilis* and *Caulobacter crescentus* (Yamaichi and Niki, 2000). While the plasmid ParA

*Corresponding author. National Institute of Genetics, Radioisotope Center, Yata 1111, Mishima 411-8540, Japan. Tel.: +81 55 981 6870; Fax: +81 55 981 6880/6871; E-mail: hniki@lab.nig.ac.jp

Received: 15 October 2003; accepted: 14 November 2003; Published online: 18 December 2003

and ParB homologs clearly have a biological function in the active partitioning of each daughter plasmid towards the daughter cells, the role of the chromosomal Par homologs in chromosome partitioning is still unclear. Curiously, members of neither family, ParA or ParB, are found in the chromosomes of *E. coli* and related bacteria.

In this paper, we analyzed the bipolar positioning of *oriC* in a systematic series of chromosomal split and deletion mutants by using fluorescent *in situ* hybridization (FISH). In addition, visualization of the nucleoids in living cells produced real-time imaging of simultaneous chromosome replication and segregation, making it possible to assay for a *cis*-acting site involved in bipolar migration of *oriC* during nucleoid division. We propose that *migS* functions as a centromere-like element for bipolar positioning of the replicated *oriC* segment.

Results

Construction of chromosomal split mutants

To identify a *cis*-acting element involved in bipolar chromosome migration, a series of mutants was created by splitting subchromosomes from the original chromosome. When moved to a separate subchromosome, the *cis*-acting function of this element will be disrupted, which may be observed as defects in chromosome migration, or positioning.

We used a variation of Itaya's method (Itaya and Tanaka, 1997), in which a plasmid is integrated into a point of interest on a chromosome by homologous recombination between two truncated antibiotic-resistant alleles (Figure 1A). The *oriC* plasmid or F plasmid can systematically be integrated into a chromosome and be used as the replication origin of a secondary chromosome. The replication origin of F plasmid was mainly used to construct a chromosomal split mutant. In addition to the replication origin, a partitioning system is essential for stably maintaining the secondary chromosome in cells. The *sopABC* genes were introduced into all the secondary chromosomes together with a replication origin.

The selected integration points for the cassettes were either in a nonessential gene or noncoding chromosome regions. None of the strains carrying integrated cassettes showed any defects in cell growth or subcellular distribution of nucleoids, even when the secondary replication origin was integrated into the chromosome (data not shown). We isolated two chromosomal split mutants: one split off the 480 kb chromosomal segment between 73.9 and 84.5 min (YK2005), and the other split off the 720 kb chromosomal segment between 84.7 and 0.1 min (YK2015, Figure 1B). Physical dissection of the chromosomes was confirmed by pulsed-field gel electrophoresis analysis (Supplementary Figure 1).

Bipolar positioning of *oriC* is stalled in a mutant in which a 720 kb segment is split from the chromosome

The chromosomal *oriC* segment is localized mainly at the middle of cells in cultures growing slowly, and *oriC* copies are abruptly separated after replication (Niki *et al.*, 2000). The separated *oriC* segments are localized near cell poles even in cells of unit cell length. To test for bipolar positioning defects in chromosomal split mutants, we statistically analyzed the subcellular localization of *oriC* by FISH. Normal bipolar positioning is expected to show a distinct separation of

fluorescent foci to the opposite cell poles, while defects may result in a less obvious separation of the two foci.

We tested the localization of *oriC* at the midcell in the chromosomal split mutants. The subcellular localization of *oriC* indicates that, in cells with a single *oriC* focus, the focus was localized mainly at the midcell in both wild type and the chromosomal split mutants (Figure 2A-c, B-c, C-c, and D-c).

We then analyzed the subcellular localization of *oriC* in cells with two fluorescence foci. A bipolar distribution of *oriC* was observed in both parental strains YK2012 and YK2002 (Figure 2A-a and b, and C-a and b). The bipolar distribution of *oriC* was not affected in the YK2005 mutant with a 480 kb chromosomal segment between 73.9 and 84.5 min on the genetic map (Figure 1B). The two *oriC* foci were rarely located close to each other in the middle of the cells (Figure 2D-a and b). In contrast, the bipolar distribution of *oriC* was disrupted in the YK2015 mutant with a 720 kb of chromosomal segment between 84.7 and 0.1 min (Figure 1B), as indicated by the high frequency of cells in which the two *oriC* foci colocalized in the middle of cells (Figure 2B-a and b). This disruption of bipolar positioning of *oriC* was most pronounced in smaller cells (1.5–2.0 μm of cell length in Figure 2B-a). In longer cells (more than 2.0 μm long, Figure 2B-a), the two *oriC* foci tended to be localized at/near cell quarters, suggesting that the two copies of *oriC* were separated from each other according to the cell division cycle.

To quantify the extent of the disruption of bipolar positioning of *oriC*, we utilized an index of bipolar positioning (IBP): the frequency of cells with two fluorescence foci located within the middle of cells, which was defined as the area between 35 and 65% of the cell length. The index was 8.7 in the wild-type strain (Figure 1B). In the case of the split chromosomal segment between 73.9 and 84.5 min (YK2005), the index was somewhat higher than that of the wild-type strain (Figures 1B and 2D-b). In contrast, the IBP of the mutant with the split chromosomal segment between 84.7 and 0.1 min (YK2015) was 21.8, more than double the IBP of the parental strain (Figures 1B, 2A-b and 2B-b). These results indicate that the 720 kb of the segment between 84.7 and 0.1 min contains the *cis*-acting element responsible for the bipolar positioning of *oriC* on the chromosome.

A 15 kb of chromosomal segment is common to the chromosomal split mutants with disrupted *oriC* positioning

We constructed a series of mutants with split chromosomal segments within the 720 kb between 84.7 and 0.1 min on the genetic map, and further analyzed the bipolar positioning of *oriC* in these mutant cells (Figure 1B). Eight chromosomal split mutants had a significant increase in IBP compared to the mean of IBP of the parental strains, 11.1 ± 3.6 (standard deviation, s.d.). The bipolar positioning of *oriC* was disrupted in YK2075 and YK2185 (Figure 1B); however, it was not affected in YK2065 and YK2195 (Figure 1B). These results suggest that the 15 kb of the chromosome between 89.1 and 89.5 min had an influence on the bipolar positioning of *oriC*. When only the 15 kb was split from the original chromosome, the IBP was increased from 9.1 before the splitting to 25.6 after the splitting (Figure 1B, YK2175). These data strongly indicate that the 15 kb chromosomal segment between 89.1 and 89.5 min was responsible for stalling the bipolar

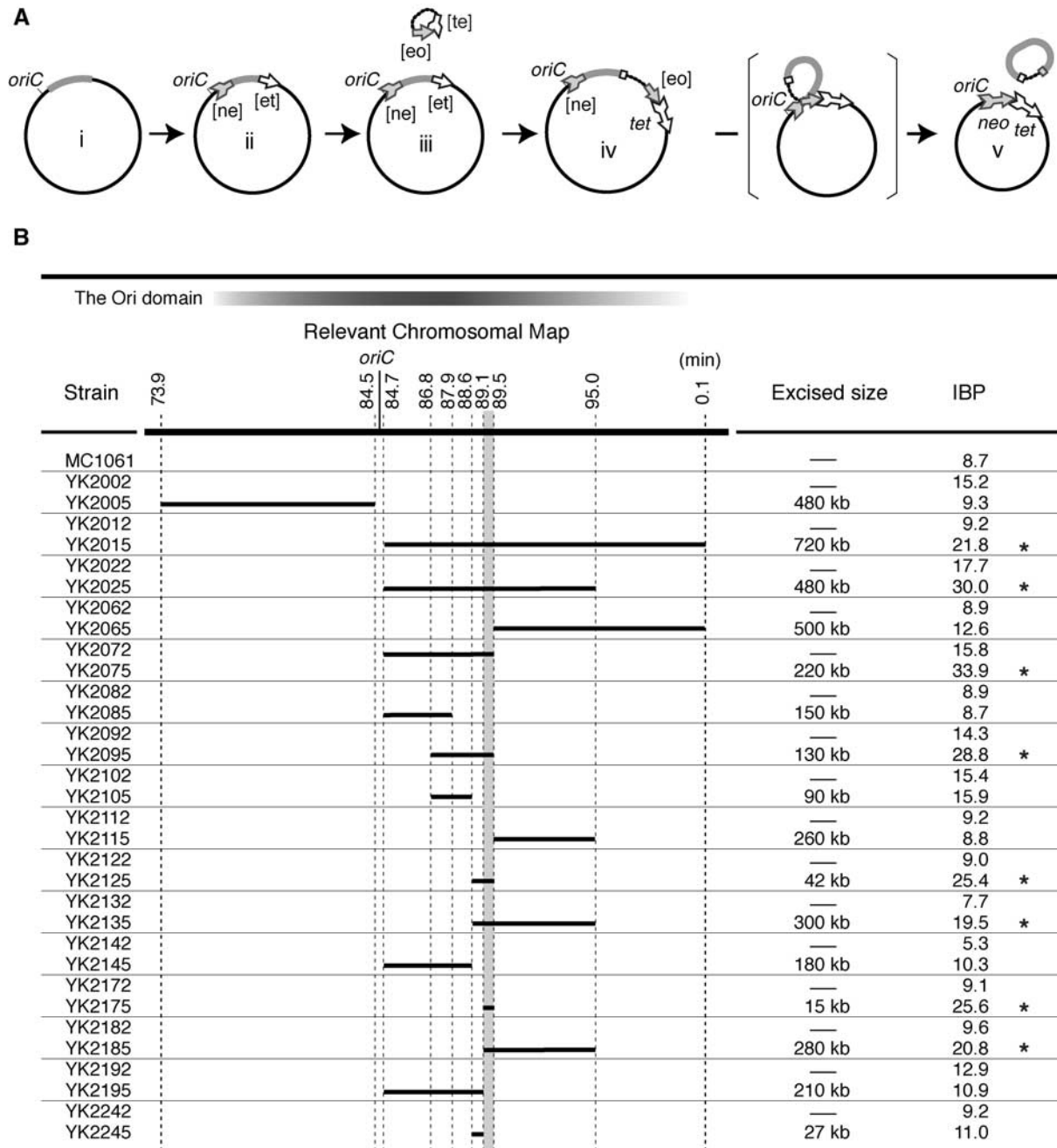


Figure 1 Construction and characterization of the chromosomal split mutants. (A) Schematic diagram of the construction of chromosomal split mutants. All chromosomal split mutants are derived from MC1061. The chromosomal segment to be excised is drawn in gray (i). The [ne] cassette (gray arrow tail) and the [et] cassette (white arrowhead) were inserted into the desired endpoints of the chromosomal segment to be excised. The [ne] cassette includes a neomycin-resistant gene (*neo*) that is deleted at the 3'-end. The [et] cassette includes a tetracyclin-resistant gene (*tet*) that is deleted at the 5'-end (ii). A low copy-number plasmid carrying both the [eo] cassette (gray arrowhead) and the [te] cassette (white arrow tail) was introduced. The [eo] cassette includes the *neo* gene that is deleted at the 5'-end. The [te] cassette is the *tet* gene that is deleted at the 3'-end (iii). Homologous recombination between the [te] and the [et] cassette generated a complete tetracyclin-resistant gene and simultaneously the plasmid was integrated into the chromosome (iv). Homologous recombination between the [ne] and the [eo] cassette generated a complete neomycin-resistant gene and simultaneously a subchromosome (v). (B) Chromosomal split mutants and their activity for bipolar migration of *oriC*. A series of chromosomal segments that were split from the original chromosome are shown as bold bars, with the *E. coli* chromosome map between 73.9 and 0.1 min (thick bold line). The chromosomal region including *oriC* nearly corresponds to the Ori domain (Niki *et al.* 2000), which is indicated in a bar above the chromosomal map. The IBP is the frequency of cells with two fluorescence foci located within the middle of cells, which was defined as the area between 35 and 65% of the cell length in arbitrary units. Asterisks indicate the chromosomal split mutants with significantly increased values in IBP, which are more than 18.7 (mean + 2 × s.d., see the text). The chromosomal segment common to the chromosomal split mutants with higher IBP is indicated in gray.

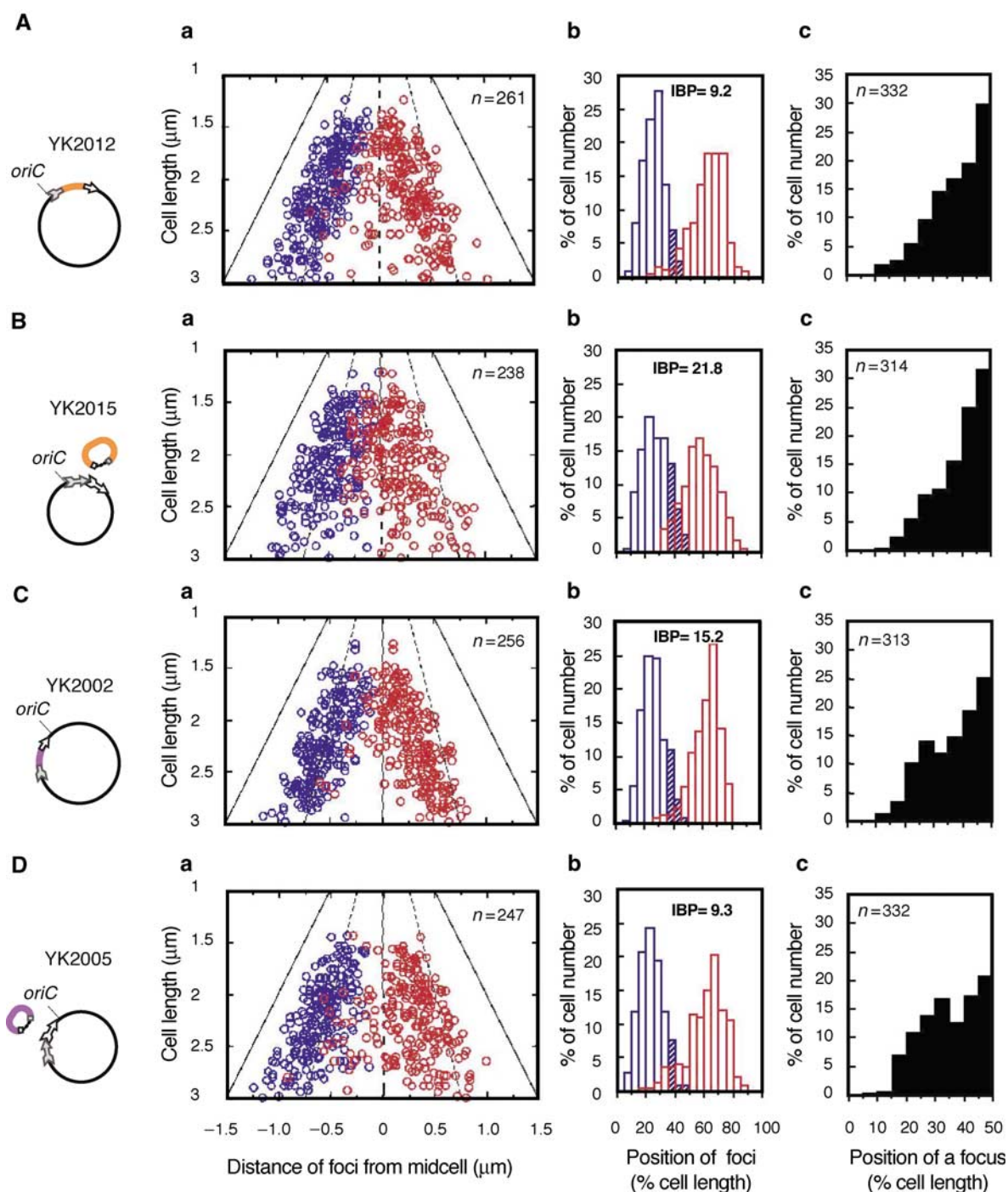


Figure 2 Subcellular localization of the *oriC* segment before or after chromosomal splitting. The *oriC* segments on the chromosome were detected by the FISH method, and the positions of *oriC* foci were measured in cells with two foci or one focus. (A) YK2012, (B) YK2015, (C) YK2002, (D) YK2005. Schematic diagrams indicate the physical state of the chromosome and the split subchromosome: split chromosomal segments (colored lines), and the cassettes (arrows). (a) Cells with two fluorescent foci were statistically analyzed. The positions of *oriC* foci from the midcell are plotted versus cell length. The focus closest to a pole is shown in blue. The distance of the other focus from the same pole was measured (red). The broken lines indicate the 1/4 and 3/4 positions of cell length, and the solid lines indicate the position of a cell pole. The thin lines indicate midcell points. (b) The histogram shows the distribution frequency of the foci. The hatched areas correspond to values of the IBP. (c) Cells with a single fluorescent focus were statistically analyzed and the distribution frequency of the foci is shown in the histogram.

positioning of *oriC*. This finding was consistent with the results in the other mutants (Figure 1B).

A 46 bp sequence is common to deletion mutants with disrupted *oriC* positioning

There are 14 genes, including those deduced from the *E. coli* genomic sequence, on the chromosome between 89.1 and

89.5 min (Figure 3C). No essential gene for cell proliferation has been mapped to this segment. We constructed a mutant with a deletion of the chromosomal segment between 89.1 and 89.5 min. The deletion mutant was isolated and able to grow on both rich and minimal medium. Surprisingly, the deletion did not cause any noticeable perturbation of cell proliferation. However, the IBP was strikingly increased from

A

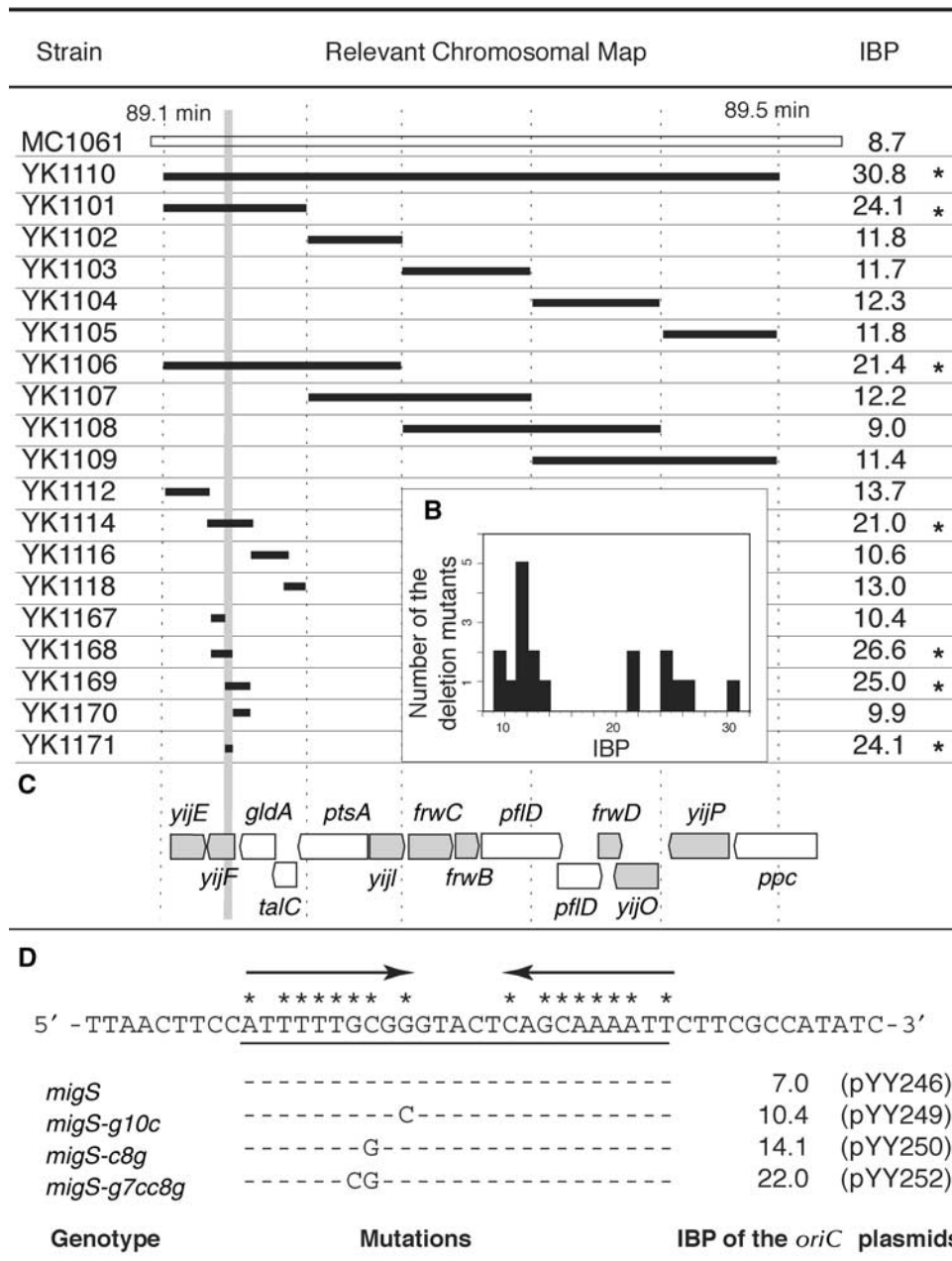


Figure 3 Bipolar positioning of *oriC* in various chromosomal deletion mutants. (A) Systematic chromosomal deletion mutants were constructed within the 15 kb segment between 89.1 and 89.5 min. Deleted segments are shown as bold bars on the chromosome map (white bar). The exact endpoints of deleted segments are described in Supplementary Table I. The chromosomal segment common to the deletion mutants with higher IBP is indicated in gray. Asterisks indicate the chromosomal split mutants with significantly increased values in IBP (see the text). (B) Histogram of the distribution frequency of the IBP among the deletion mutants. (C) Coding regions on the chromosomal segment between 89.1 and 89.5 min. Genes estimated from the nucleotide sequence are indicated in gray. (D) The deleted chromosomal segment in YK1171 is a 46 bp nucleotide sequence. Arrows indicate an imperfect inverted repeat. Matched nucleotides are shown by an asterisk. Point mutations are shown with the IBP of the *oriC* plasmids that have the corresponding *migS* sequence with or without the mutations.

8.7 to 30.8 (Figure 3A; MC1061 and YK1110), indicating that bipolar positioning of *oriC* was inhibited in the deletion mutant. Next, we constructed a series of systematic deletion mutants within the chromosomal segment between 89.1 and 89.5 min (Figure 3A). To evaluate defects in bipolar positioning of *oriC* in these deletion mutants, we referred to the mean of IBP of the chromosomal split mutants with defects in *oriC*

positioning in Figure 1B (25.7, s.d. = 5.0). An IBP higher than 20.7 (mean - s.d.) was considered to be a significant defect in the bipolar positioning of *oriC*. This estimation is consistent with the distribution of IBP in the deletion mutants (Figure 3B).

We found that bipolar positioning of *oriC* was disrupted in two deletion mutants, YK1101 and YK1106, but not in the

other mutants (Figure 3A). Therefore, we further constructed nine deletion mutants within the chromosomal segment common to YK1101 and YK1106. In four of these deletion mutants (YK1114, YK1168, YK1169, and YK1171), the IBP was over 20.7, and the IBP in the remaining mutants was less than 15.7 ($25.7 - 2 \times \text{s.d.}$). The common segment in the four deletion mutants that showed disruption in bipolar positioning is only 46 bp and is located within a coding region, *yijF*, deduced from the genomic sequence (Figure 3C). The YK1167 deletion mutant had a 247 bp of deletion within the *yijF* gene, but no increase in the IBP (Figure 3A), suggesting that the encoded product was not involved in the bipolar positioning of *oriC*. The analyses with systematic deletion mutants defined a 46 bp sequence including an imperfect 10 bp inverted repeat with a 5 bp spacer as a *cis*-acting site on the bipolar positioning of *oriC* on the chromosome (Figure 3D).

A mutation in the plasmid partitioning system stalls bipolar migration of plasmid DNA

An *oriC* plasmid including the *sopABC* partitioning system is stably maintained in host cells (Ogura and Hiraga, 1983) and localized in cell quarters throughout the cell division cycle (Niki and Hiraga, 1999). The IBP of plasmid DNA with the *sopABC* partitioning system was 7.5 (Figure 4A-a and b), being consistent with regular localization at 25 and 75% of cell length (Figure 4F, Type I). However, the IBP of an *oriC* plasmid without the *sopABC* partitioning system was similarly low (8.5). In this case, each plasmid DNA was randomly localized within the cytosolic region at cell poles and/or the midcell (Figure 4D; Niki and Hiraga, 1999), and much less colocalized at the middle of cells (Figure 4F, Type II). In contrast, an *oriC* plasmid with a mutant *sopA* ($\Delta\text{sopAsopB}^+\text{C}^+$, pXX206) had an increased IBP (about three fold) compared to the *oriC* plasmids with and without the *sopABC* partitioning system (Figure 4B-a and b). The two *oriC* foci of pXX206 were broadly distributed on the periphery of 25 and 50% of cell length compared to 25 and 75% in an actively partitioning *oriC* plasmid (Figure 4B-b). In addition, a single focus was localized at the midcell, similar to an actively partitioning *oriC* plasmid (Figure 4B-c). Plasmids with a mutant *sopB* ($\text{sopA}^+\text{B}^-\text{C}^+$) were not localized at cell quarters at all (data not shown), nor were plasmids lacking the *sopABC* genes. These results suggest that defects of the *sopA* gene inhibited bipolar migration of the plasmid from the midcell to the 1/4 and 3/4 positions, but the plasmid can still localize at cell quarters via the *sopBC* genes (Figure 4F, Type III).

The 46 bp segment rescues bipolar migration of plasmid DNA with a mutation in the plasmid partitioning

If the 46 bp segment is involved in bipolar migration of DNA in a cell, it would be interesting to test whether the *cis*-acting site for bipolar migration of *oriC* can compensate for the defect in bipolar migration of the *oriC* plasmid with $\Delta\text{sopAsopB}^+\text{C}^+$. The 46 bp sequence was inserted into the *oriC* plasmid, pXX206, and the subcellular localization of the resulting plasmid DNA pYY233 was analyzed. In cells with two fluorescence foci, each focus of pYY233 was mainly localized at 25 and 75% of cell length, similar to an actively partitioning *oriC* plasmid (Figure 4C-a and b). Moreover, the IBP of pYY233 was significantly decreased from 25.7 to 6.6 by

the addition of the 46 bp sequence. These results confirm the active role of the 46 bp sequence in the bipolar migration of DNA (Figure 4F, Type I).

A 25 bp sequence is sufficient for bipolar migration of plasmid DNA

In the plasmid partitioning systems *sopABC* and *parABS*, an inverted repeat is included in the *cis*-acting sequence, which plays a central role in the recognition of a binding protein (Davis and Austin, 1988; Mori *et al.*, 1989). We hypothesized that the imperfect 10 bp inverted repeat and 5 bp spacer would be important in the 46 bp sequence (Figure 3D). To test this possibility, the 25 bp sequence including the imperfect 10 bp inverted repeat and 5 bp space was inserted into the *oriC* plasmid with $\Delta\text{sopAsopB}^+\text{C}^+$ (pXX206). In the resulting construct, pYY246, the IBP was similar to the *oriC* plasmid containing the 46 bp sequence (Figure 3D).

To confirm that the 10 bp inverted repeat and 5 bp spacer are essential for bipolar migration, we analyzed 25 bp synthesized sequences with mutations in the inverted repeat. In mutations in which a single base in the inverted repeat was substituted (Figure 3D, *migS-g10c* and *migS-c8g*), small increases of the IBP were detected in pYY249 and pYY250 when compared to pYY246 (Figure 3D). We introduced double base substitutions into the inverted repeat, resulting in the loss of two G:C base pairs (*migS-g7cc8g*). The *oriC* plasmid pYY252 had a higher value in IBP when compared to pYY246 (Figure 3D), suggesting that *migS-g7cc8g* lost its ability to compensate inadequate migration by $\Delta\text{sopAsopB}^+\text{C}^+$ genes. Taken together, these data suggest that the 25 bp sequence represents the *cis*-acting element for bipolar migration of plasmid DNA. Therefore, we named the 25 bp sequence *migS* (for **m**igration **s**ite).

***migS* is not sufficient for specific subcellular localization of plasmid DNA**

When *migS* is carried on pXX230, that is, the *oriC* plasmid lacking the *sopABC* genes, the stability of the plasmid pYY265 does not improve at all (data not shown) and the plasmid DNA is distributed randomly in the cytosol (Figure 4E and F, Type II), as is the *oriC* plasmid lacking the *sopABC* genes (Figure 4D and F, Type II). Hence, *migS* is unlikely to be involved in the positioning of plasmid DNA at specific subcellular regions.

migS* functioning is independent of its location relative to *oriC

migS is located at 89.1 min of the genetic map, which is 211 kb from *oriC* in the clockwise direction (Figure 5A). To test the effects of the chromosomal position of *migS* relative to *oriC*, we reintroduced the 46 bp of the *migS* segment into the *migS* deletion mutant YK1143. The *migS* segment was inserted at the 80.0 min position of the chromosome, which is 211 kb from *oriC* in the counterclockwise direction (Figure 5A), and contains the *bisC* gene which is dispensable for cell growth. The IBP was 23.5 in the *migS* deletion mutant, YK1143, and 10.3 in the transferred mutant, YK1165 (Figure 5B), suggesting that this transfer of *migS* improved the bipolar positioning of *oriC* on the chromosome.

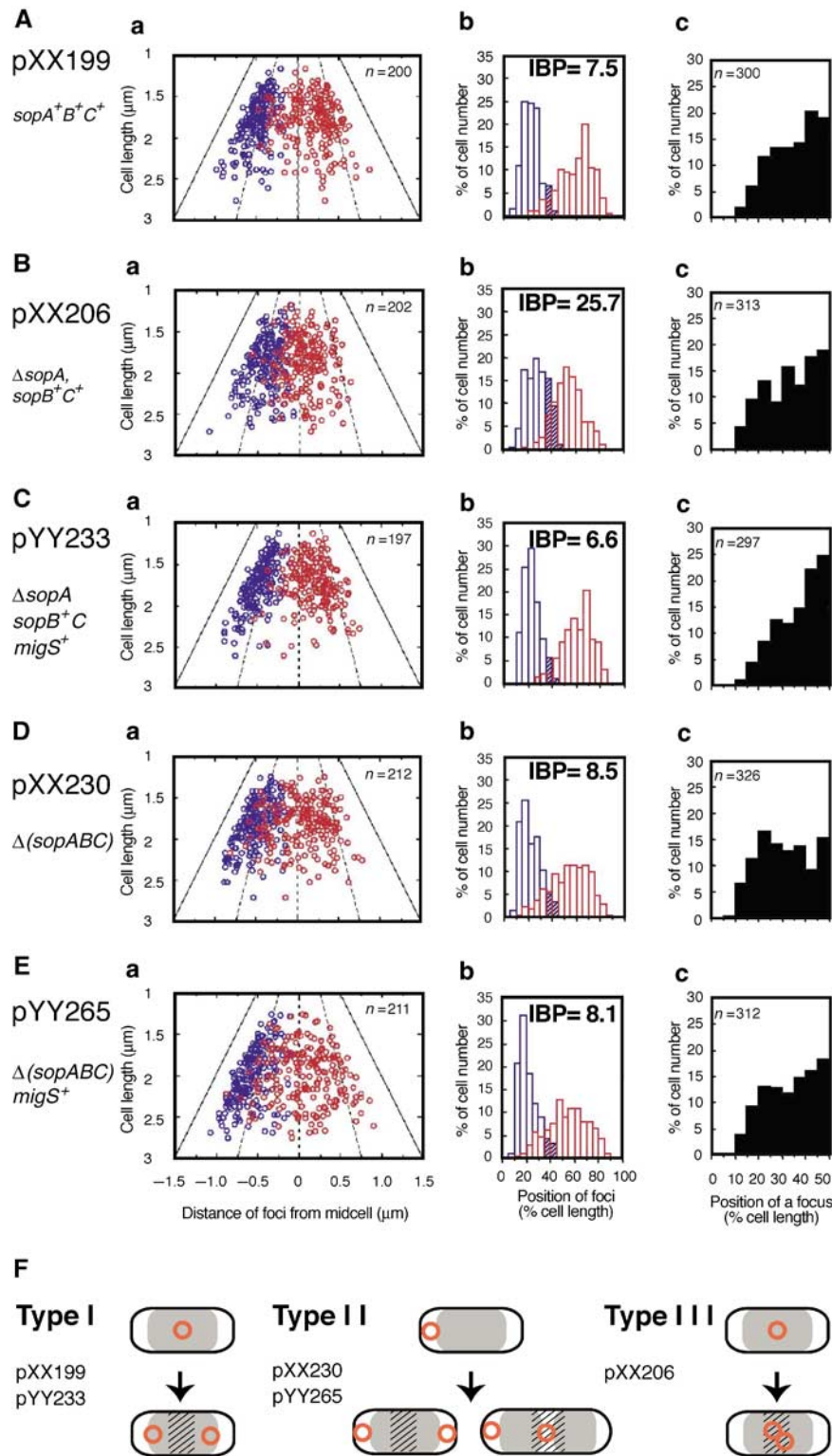


Figure 4 Subcellular localization of the *oriC* plasmids. The positions of fluorescent foci were measured in cells with one focus or two foci of various *oriC* plasmids: (A) pXX199, (B) pXX206, (C) pYY233, (D) pXX230, (E) pYY265. Cells with two fluorescent foci were statistically analyzed. The positions of fluorescent foci are shown by scatter diagram (a) or histogram (b) as described in Figure 2. (c) Cells with one fluorescent focus were statistically analyzed and the distribution frequency of the foci is shown in the histogram. (F) Schematic diagrams indicate the subcellular localization patterns of plasmid DNA molecules (circles) in a cell: nucleoids (gray) and subcellular areas that are 35–65% of the cell length (hatch).

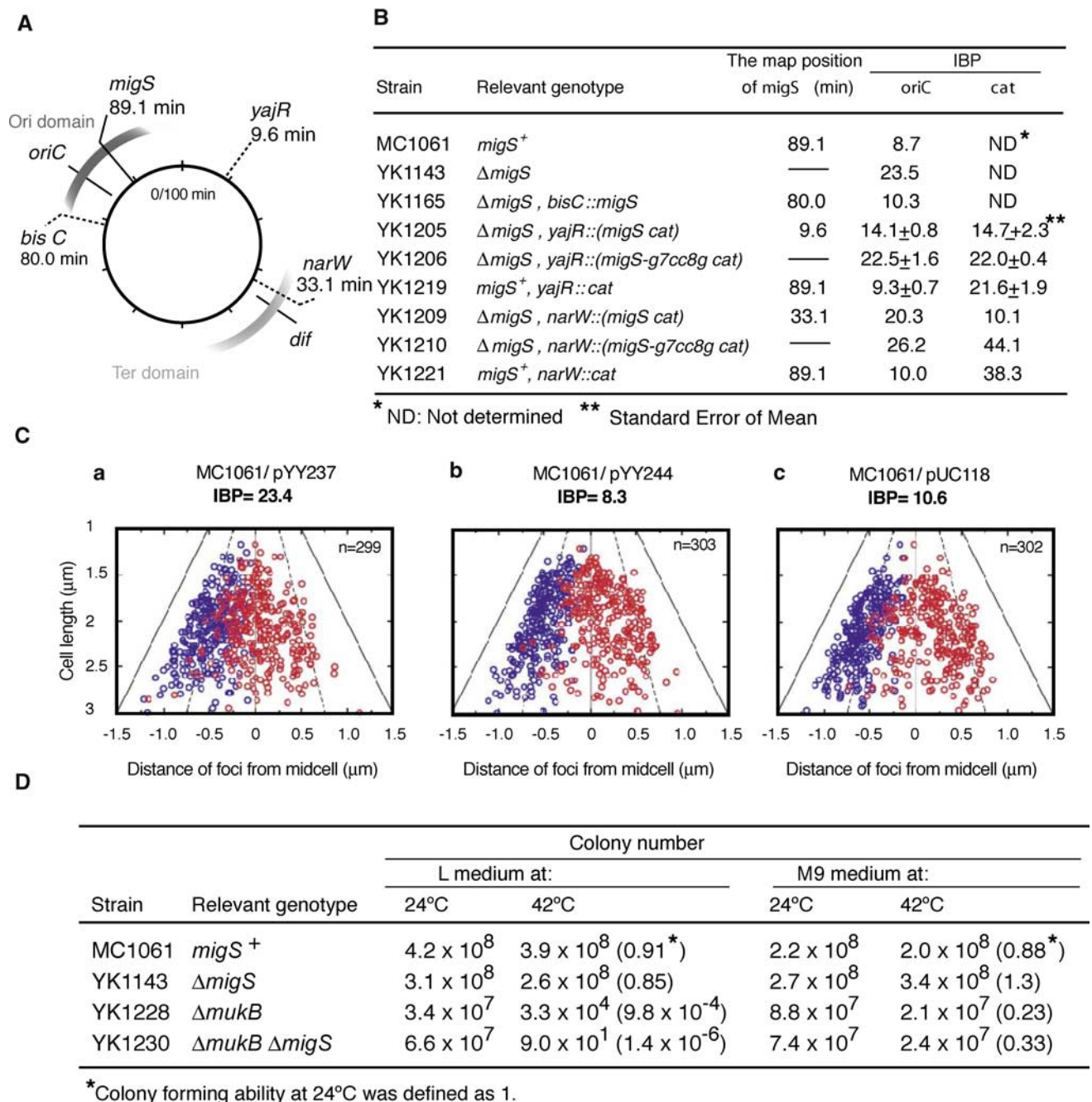


Figure 5 Characterization of *migS*. (A) A map indicates various chromosomal locations where *migS* is placed on. (B) Effect of placed *migS* on bipolar positioning of the chromosomal segment. The IBP of *oriC* on the chromosome and the chromosomal segment including the *cat* gene are indicated. The standard errors were calculated on three independent experiments. (C) Effect of high copy-number *migS* plasmid on bipolar positioning of *oriC* on the chromosome. The positions of *oriC* foci were measured in cells with two fluorescent foci and shown by scatter diagram: (a) cells harboring pYY237 (*migS*); (b) cells harboring pYY244 (*migS-g7cc8g*); (c) cells harboring pUC118 (a vector). (D) Colony-forming ability of a cell with the double null mutations of *mukB* and *migS*, depending on growth temperature and culture medium.

Bipolar positioning of the replication terminus under the control of *migS*

The replication terminus of *E. coli* and the large flanking region, the Ter domain, are localized in the middle of the cell until completion of chromosome replication (Niki and Hiraga, 1998; Niki *et al.*, 2000). This explains the rather high IBP for the replication terminus when assayed by FISH (Figure 5B, YK1221). The chromosomal segment that lies between the Ori and the Ter domain is not localized at a

specific subcellular position during the cell cycle (Niki *et al.*, 2000), and the IBP of this chromosomal segment was between those at the Ori and the Ter domain (Figure 5B, YK1219).

To further investigate the observed position effect of *migS*, it was placed at various chromosomal locations in combination with a reporter gene, *cat*. We used the *cat* gene as the FISH probe to detect the chromosomal location. We transferred 25 bp of *migS* with the *cat* gene to 9.6 or 33.1 min on

the chromosome (Figure 5A). When *migS* was located at an intermediate chromosomal position (9.6 min), the IBP for *cat* decreased slightly, but significantly, from 22.0 ± 0.4 (YK1206) to 14.7 ± 2.3 (YK1205). Bipolar positioning of *oriC* was also improved by placement at this position (Figure 5B). On the other hand, placement of *migS* at the replication terminus (33.1 min) strikingly decreased the IBP for *cat* from 38.3 to 10.1 (Figure 5B, YK1209 and YK1221), but the IBP of *oriC* was not improved at all (Figure 5B, YK1209 and YK1210). These results indicate that *migS* functions as a mediator for the bipolar positioning of replicated chromosome segments, independent of chromosomal location. This positional effect of *migS* on bipolar positioning was especially remarkable at the chromosomal location within the Ter domain (33.1 min), which normally does not segregate until the very end of chromosome replication.

Multiple copies of *migS* stall bipolar positioning of *oriC*

We cloned 46 bp of the *migS* segment in a high copy-number plasmid and tested the effect of multicopy *migS* on the bipolar positioning of *oriC*. The IBP was markedly increased (Figure 5C-a), similar to the *migS* deleted mutant (Figure 5B; YK1143). Thus, multicopy *migS* cancelled the bipolar positioning of the *oriC* segment on the chromosome. However, multiple copies of a mutated *migS* sequence did not affect the bipolar positioning of *oriC*, and the index was as low as that of the vector plasmid (Figure 5C-b and c).

The *migS* null mutation enhances temperature-sensitive lethality of the *mukB* null mutation

The *E. coli mukB* gene is involved in faithful chromosome segregation. The null mutant can grow at low temperature, producing anucleated cells in high frequency, but does not grow at high temperature on L medium (Niki *et al.*, 1991). As cell division is strongly inhibited in *mukB* null mutants at a high temperature, filamentous cells are produced. We constructed a *mukB* null mutant (YK1228) that was derived from the wild-type strain MC1061. This strain produced anucleated cells (Supplementary Figure 2), could not grow at high temperature depending on culture medium (Figure 5D), and produced filamentous cells at a restricted condition (Supplementary Figure 2).

To analyze the effects of the *migS* null mutations on the medium-dependent, temperature-sensitive, lethal phenotype of the *mukB* null mutation, we introduced the *migS* null mutation into the *mukB* null mutant. *migS* and *mukB* double mutants could grow on both the M9 and L medium at 24°C and produced a high frequency of anucleate cells similar to the *mukB* null mutant (Supplementary Figure 2). The colony-forming ability of the double null mutant decreased remarkably at high temperature on L medium (Figure 5D). No filamentous cells were detected in the double null mutants at high temperature on L-medium, suggesting quick inhibition of cell elongation at restricted temperature (Supplementary Figure 2). These results suggest that the bipolar positioning of *oriC* by *migS* can interact with the biological function of the *mukB* gene.

Dynamics of morphological changes disappear in the *migS* deletion mutant

Anucleated cells were not observed at a significant frequency in the *migS* deleted mutant. Also, there was no remarkable

difference of the doubling time between the wild type (MC1061: 70 min) and the *migS* deleted mutant (YK1143: 73 min) in minimal medium at 37°C. To confirm the effect of *migS* on chromosome distribution, we analyzed the morphological changes of nucleoids in a living cell with or without *migS* during the process of chromosome replication and segregation. We used a gelatin mounting method to observe the nucleoids in living mutant cells (Manson and Powelson, 1956).

Nucleoids in living cells mounted in 23% gelatin-containing culture medium show a remarkable contrast with the cytosol under a phase-contrast microscope. When cells in gelatin-containing M9 medium were grown at 30°C, nucleoids in both wild type and the *migS* null mutant were ellipse or oval throughout the cell division cycle (Figure 6A-a and b). In wild type, elongated cells (>2 μm) without

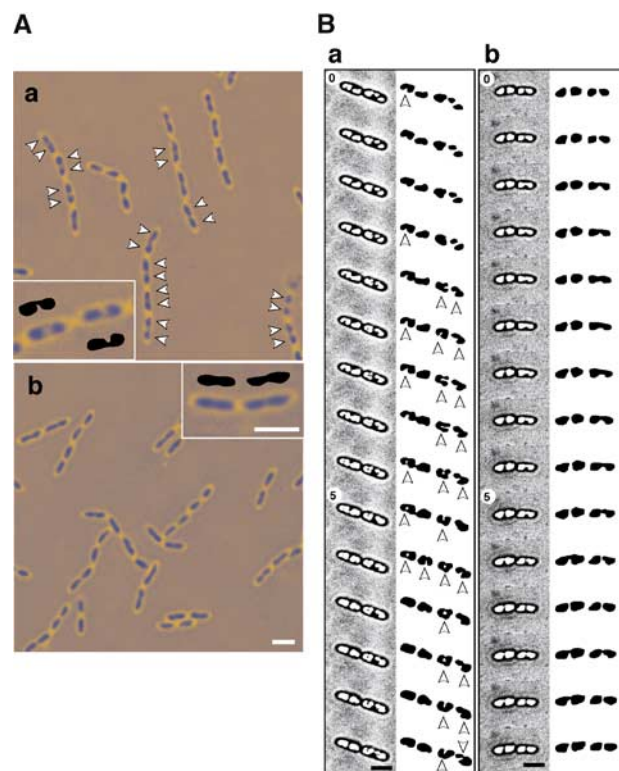


Figure 6 Microscope images of a living cell in gelatin-containing medium. (A) Nucleoids in cells were grown to mid-log phase at 30°C in M9 medium. Living cells were mounted in 23% gelatin-containing medium to detect chromosomal DNA. Cells were shown in phase-contrast images with pseudo-coloring. (a) MC1061 (wild type), (b) YK1143 ($\Delta migS$). Arrowheads indicate two discrete nucleoids in an elongated cell (>2 μm) without constriction. Typical nucleoids in an elongated cell (>2 μm) without constriction were indicated in inside panels with diagrams of extracted nucleoids. Scale bar represents 2 μm. (B) Time-lapse microscopy of a living cell mounted in gelatin. Cells pre-incubated in L medium with 0.2% glucose at 30°C were transferred to a dish with a coverslip and mounted in 23% gelatin-containing L medium with 0.2% glucose. The phase-contrast pictures were taken at 30 s intervals: (a) MC1061 (wild type), (b) YK1143 ($\Delta migS$). The numbers correspond to minutes in the frames of time-lapse imaging. The images were improved in the nucleoid outline using the “equalization” treatment of Adobe Photoshop ver. 7. Extracted nucleoids are shown as diagrams on the right side with magnification (1.5 ×). Arrowheads indicate lobed nucleoids. The original images were shown in Supplementary Figure 3. Scale bar represents 2 μm.

constriction for cytokinesis have two discrete nucleoids, which look like beans in a pod (Figure 6A-a). In the *migS* null mutant, such elongated cells have elongated ellipse nucleoids that are divided according to cytokinesis (Figure 6A-b).

These differences in nucleoid shape between wild type and the *migS* null mutant are more apparent in the fast growing conditions. A variety of nucleoid shapes appeared in an actively dividing wild-type cell when cells in gelatin-containing L medium were grown at 30°C (Figure 6B-a). The division time was about 30 min, suggesting that multi-fork replication should be occurring. There were four nucleoids in almost all cells with constrictions at the midcell. After the separation of sister nucleoids, the shape of the nucleoids quickly changed to lobed or dumbbell form for a few minutes. Depending on the stage in the cell division cycle, nucleoids were elongated and more distinctly lobed. In contrast, the change in nucleoid shape was poor in the *migS* deleted cells, despite the almost same dividing time (Figure 6B-b). After separation of the sister nucleoids, four nucleoids in a single cell gradually increased in size. The shape was round or ovoid throughout the cell division cycle. The observation suggests that bipolar positioning of the *oriC* segment inside a nucleoid may contribute to reorganization of the replicated daughter strands that are positioned in a bipolar manner.

Discussion

In this paper, we have identified a 25 bp sequence, *migS*, which plays a crucial role in the bipolar positioning of the *oriC* segments during chromosome partitioning in *E. coli*. The plasmid without the SopABC partitioning system was not found to localize at specific subcellular sites, even when harboring active *migS*. Therefore, we proposed that *migS* is responsible for the bipolar migration of *oriC* and the flanking region rather than subcellular positioning (Figure 7), and suggest that *migS* functions as a centromere-like element in bacteria.

migS may play a role in the organization of replicated daughter chromosomes in duplicating cells (Figure 7). Active migration of *oriC* and the flanking region establishes the bipolar positioning of replicated daughter chromosomes at an early stage in chromosome replication, and the bipolar positioning may promote compaction of replicated daughter chromosomes to make discrete nucleoids as shown in Figure 6. During the process of nucleoid formation, MukB protein, a bacterial member of SMC family, plays a central role in chromosome folding. Deterioration in the temperature-sensitive growth of the *migS* and *mukB* double null mutant suggests direct interaction between *MukB* and bipolar positioning by *migS* during chromosome partitioning. As bipolar positioning, or separation, of the replicated chromosomal segments helps to make discrete nucleoids at an early stage of the cell division cycle, the double null mutant may have severe damage on nucleoids formation of newly replicated chromosomes.

Such a scenario would allow *migS* to play a role in chromosome organization. However, insertion of *migS* near the replication terminus drastically changes the positioning of this region, supporting a model in which *migS* is directly involved in chromosome orientation including positioning and migration.

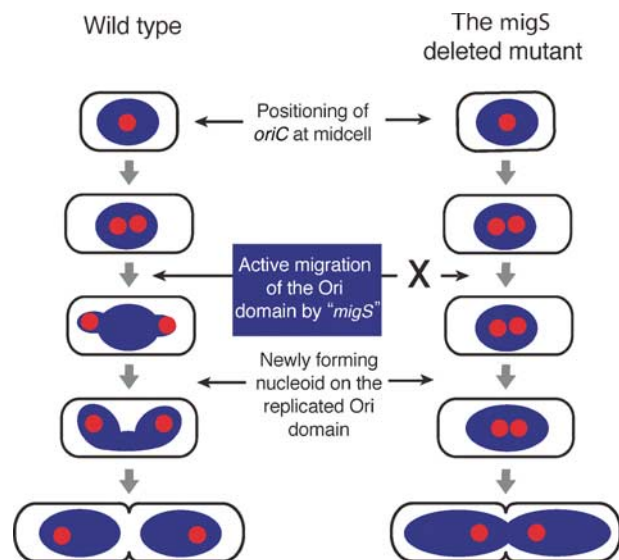


Figure 7 Model of the *oriC* bipolar migration/positioning and nucleoids formation. In a wild-type cell growing slowly, the *oriC* segment is replicated at midcell. The replicated *oriC* segments migrate towards the cell quarters, dependent on the function of *migS* located near *oriC*. After migration by *migS*, the Ori domains of the chromosome including the replicated *oriC* segment and the adjacent chromosomal segments localize at or near the cell quarters. The Ori domains are newly folded to make discrete sub-nucleoids, and a whole nucleoid looks like a dumbbell. The highly organized chromosome structure is presumably involved in tethering the Ori domain at or near the cell quarters. On the other hand, in the *migS* deleted mutant, bipolar positioning of the replicated *oriC* segments is defective because of the loss of putative active migration by *migS*. As the replicated *oriC* segments and the adjacent chromosomal segments still localize at the midcell, newly forming nucleoids are not discrete. However, the chromosome condensation by the MukB protein at the cell quarters (Ohsumi *et al.*, 2001) may compensate for the defect in the formation of discrete nucleoids, and nucleoids are clearly separated before septum closing. The shared masses represent the *E. coli* nucleoids, or organized chromosomes in a cell; red circles indicate replication origin, *oriC*. *migS* is located near *oriC*.

The location of *migS* is 211 kb from *oriC* in the clockwise direction, in the middle of the Ori domain. The timing of initiation of bipolar migration of the *oriC* segment may be related to the distance between *oriC* and *migS* on the chromosome. Placement of the 46 bp sequence including *migS* restores normal bipolar positioning of *oriC*. Moreover, placement of 25 bp *migS* at other locations causes bipolar positioning of the chromosomal segment at the placed location including the replication terminus. Therefore, the 25 bp sequence of *migS* is sufficient to induce its *cis*-acting effect on bipolar positioning of the chromosome. The *oriC* sequence is not essential for bipolar positioning of the chromosome, and the distance of *migS* and *oriC* is not involved in bipolar positioning of the chromosome.

In the absence of *migS*, the Ori domain can still be found localized to the midcell before replication (Figure 2B). pYY265, an *oriC* plasmid with only *migS*, is still distributed randomly in the cytosol and cannot localize at specific cellular sites (Figure 4E). Clearly, the *migS* site does not tether DNA to any specific site in a cell, other than carrying out bipolar migration of DNA. This is consistent with our results that the *oriC* segment on the chromosome

in the *migS* deleted cells can still localize at midcell before replication (data not shown). In addition, the chromosomal split mutants within the Ori domain can also localize at midcell before replication (Figure 2), suggesting that there is no specific sequence for tethering the Ori domain including *oriC* at/near the cell quarters. When *migS* is simply involved in the migration of chromosomal segments, static localization of the *oriC* segment at the cell quarters is probably dependent on chromosome organization with high-order structure, rather than a specific sequence.

Analogous to the ParAB partitioning system, some proteins may bind to the inverted repeat sequence of *migS*. The *migS* sites on the high copy-number plasmid abolish bipolar migration of *oriC* on the chromosome, presumably because the *migS* sites compete with one another to bind a *trans*-acting factor involved in *oriC* migration. Significantly, the base mutations in the inverted repeat of *migS* cancel the multicopy effect completely. Thus, the multicopy effect of *migS* on the bipolar migration of *oriC* on the chromosome strongly supports the above hypothesis.

The *migS* sequence is unique in the *E. coli* genome. We could not find the *migS* sequence or homologs on other bacterial genomes in DNA databases. The *migS* sequence is located within a coding region, the *yijF* gene that codes for a 23 kDa hypothetical protein. Homologs of the *yijF* gene are conserved in the genomes of *Salmonella typhimurium*, *Pseudomonas aeruginosa*, *Pasteurella multocida*, and *C. crescentus*. However, homologous sequences of *migS* and a similar inverted repeat have not been found in these coding regions of the *yijF* gene homologs.

There are marked differences in subcellular localization between plasmids defective in different *sop* genes (Figure 4F). Plasmids defective in either *sopA* or *sopB* are easily segregated from host cells, and both frequencies of plasmid loss are as high as that of plasmids without the *sopABC* genes (Ogura and Hiraga, 1983). In the case of the plasmid with $\Delta\text{sopAsopB}^+\text{C}^+$, the plasmid could be localized at midcell. Possibly, SopB could bind to the *sopC* site to form the SopB–*sopC* complex. We consider that the SopB protein in the complex is a mediator in order to attach plasmid DNA to a specific cellular site at the midcell, and SopA would be responsible for the release of plasmid DNA from SopB–*sopC* complexes (Libante *et al.*, 2001).

The plasmid with $\Delta\text{sopAsopB}^+\text{C}^+$ can be localized at the midcell, but not at the 1/4 and 3/4 positions of cell length regularly. We speculated that the plasmid with $\Delta\text{sopAsopB}^+\text{C}^+$ is defective in the migration of plasmid DNA from the midcell to the 1/4 and 3/4 positions during plasmid partitioning. We then demonstrated that the defect is rescued by the *migS* sequence on the plasmid with the $\Delta\text{sopAsopB}^+\text{C}^+$ genes. However, the stability of the mutated plasmid with *migS* was not recovered to the wild-type level. The pYY233 plasmid was as readily segregated from a host cell in nonselective medium as the plasmid lacking the *sopABC* partitioning genes (data not shown). When the pYY233 plasmid was transformed into the strain in which the 46bp sequence was deleted on the chromosome, the stability of the pYY233 plasmid had no increase compared to that in wild-type cells (data not shown). Our FISH analyses indicate that the localization pattern of plasmid DNA molecules in cells with one or

two fluorescence foci does not reflect the frequency of cells harboring plasmid DNA molecules. Therefore, it is likely that most plasmid DNA molecules still remained at the midcell despite *migS* addition, and the bipolar migration by *migS* is not coupled to the release of plasmid DNAs from the SopB–DNA complexes at midcell, or an enough motive force for it.

A bacterial chromosome in a living cell is highly compacted with organized structure. The compacted chromosome, or nucleoid, has been observed in fixed cells under the fluorescence microscope by using a DNA-specific fluorescence dye, DAPI. An alternative method of observing a nucleoid in the cell is the gelatin mounting method under phase-contrast microscopy. This age-old method makes it possible for us to capture dynamic changes in replicating and segregating chromosomes in real time. Clear, sharp images of a nucleoid have revealed that active bipolar migration by *migS* contributes to nucleoid morphology in a dividing cell. This method also reveals that the dynamics of nucleoids are dependent on growth condition. In addition to *E. coli*, the nucleoids of *B. subtilis* are clearly visible in living cells (H Niki, unpublished data). Hence, this method will further be applied to demonstrate nucleoid dynamics in various mutants and bacteria.

Although the *migS* sequence may play a crucial role in the bipolar migration and positioning of *oriC*, the deletion does not cause any severe defects in chromosome partitioning. It is a seemingly unnecessary process for bacterial segregation. Nevertheless, bipolar migration and positioning by *migS* presumably helps accurate chromosome partitioning. The current view indicates that bacterial chromosome partitioning consists of a series of processes, including *oriC* migration, chromosome condensation, localization of the replication machinery, and chromosomal resolution (Lemon and Grossman, 2001; Sawitzke and Austin, 2001). Genes involved in the process of chromosome condensation or compaction have been identified: *mukB* (Niki *et al.*, 1991) and *seqA* (Hiraga *et al.*, 1998). These genes are not essential for cell growth, and the *mukB* and *seqA* genes are dispensable for chromosome partitioning when suppressed by mutations in other genes (Weitao *et al.*, 1999; Sawitzke and Austin, 2000). Moreover, the replication machinery and condensation proteins presumably migrate from the midcell to the 1/4 and 3/4 positions, independently of *oriC* migration (Hiraga *et al.*, 1998; Lemon and Grossman, 1998; Ohsumi *et al.*, 2001). Taken together, we speculate that the function of the various processes in chromosome partitioning overlap one another to some extent. In fact, deterioration in the temperature-sensitive growth of the *migS* and *mukB* double null mutant supports interaction between the MukB protein and bipolar migration of *migS* during the process of chromosome condensation, or nucleoid formation (Figure 7). The redundancy in the partitioning mechanism allows chromosome segregation with high fidelity during the bacterial cell division cycle without apparent checkpoints as in the eukaryotic cell cycle. Further work will be required to learn how *migS* contributes to chromosome partitioning. However, the *migS* sequence governing bipolar positioning of *oriC* would seem to be a new clue for identifying the whole process of bacterial chromosome partitioning.

Materials and methods

Strains, Plasmids, and Media

The principal bacterial strains and plasmids used in this study are listed in Table I. All *E. coli* strains and plasmids are listed in Supplementary Table I and Table II. Cells were grown in L broth or M9 medium supplemented with sodium succinate (0.25%), thiamine (1 µg/ml), leucine (50 µg/ml), and Casamino acids (0.4%). The following antibiotics were added to the medium when necessary: ampicillin (20 or 100 µg/ml), chloramphenicol (15 µg/

Table I Bacterial strains and plasmids used in this study

<i>E. coli</i> strain ^a	Relevant genotype
MC1061	Wild-type (F ⁻ Δ lacX74 <i>rpsL araD139</i> Δ (<i>ara leu</i>)7697 <i>galU galK hsdR mcrB thi</i>)
YK1031	<i>yrdD</i> ::[ne] <i>gidA</i> ::[et]
YK1039	<i>kup</i> ::[ne] <i>b0005</i> ::[et]
YK1142	Δ <i>migS</i> :: <i>cat</i>
YK1143	Δ <i>migS</i>
YK1165	Δ <i>migS bisC</i> :: <i>migS</i>
YK1205	Δ <i>migS yajR</i> ::(<i>migS cat</i>)
YK1206	Δ <i>migS yajR</i> ::(<i>migS-g7cc8g cat</i>)
YK1209	Δ <i>migS narW</i> ::(<i>migS cat</i>)
YK1210	Δ <i>migS narW</i> ::(<i>migS-g7cc8g cat</i>)
YK1219	<i>yajR</i> :: <i>cat</i>
YK1221	<i>narW</i> :: <i>cat</i>
YK1228	Δ <i>mukB</i> :: <i>cat</i>
YK1230	Δ <i>mukB</i> :: <i>cat</i> Δ <i>migS</i> :: <i>kan</i>
YK2002	<i>yrdD</i> ::[ne] <i>gidA</i> ::[et]/pYY159
YK2005	Δ (<i>yrdD-gidA</i>)::(<i>neo tet</i>)/pYY159[<i>yrdD-gidA</i>] ^b (derived from YK2002)
YK2012	<i>kup</i> ::[ne] <i>b0005</i> ::[et]/pYY159
YK2015	Δ (<i>kup-b0005</i>)::(<i>neo tet</i>)/pYY159[<i>kup-b0005</i>] ^b (derived from YK2012)
<i>Plasmid</i>	<i>Relevant characteristics</i>
pBEST518	<i>bla</i> [ne] (Itaya and Tanaka, 1997)
pBEST524B	<i>bla</i> [eo] (Itaya and Tanaka, 1997)
pKD3	<i>bla cat</i> (Datsenko and Wanner, 2000)
pXX199	<i>bla sopA⁺B⁺C⁺</i> (<i>oriC</i> plasmid, Ogura and Hiraga, 1983)
pXX206	<i>bla ΔsopAsopB⁺C⁺</i> (<i>oriC</i> plasmid, Ogura and Hiraga, 1983)
pXX230	<i>bla Δ(sopABC)</i> (<i>oriC</i> plasmid, Ogura and Hiraga, 1983)
pXX704	<i>bla sopA⁺B⁺C⁺</i> (mini-F plasmid, Niki and Hiraga, 1997)
pXX705	<i>bla Δ(sopABC)</i> (mini-F plasmid, Niki and Hiraga, 1997)
pYY145	<i>bla</i> [et] (see Supplementary data)
pYY154	<i>cat</i> [eo] [te] (see Supplementary data)
pYY159	pXX704 [eo] [te]
pYY233	pXX206 <i>migS</i> (46 bp DNA fragment including <i>migS</i>)
pYY237	pUC118 <i>migS</i> (46 bp DNA fragment including <i>migS</i>)
pYY244	pUC118 <i>migS-g7cc8g</i> (46 bp DNA fragment including <i>migS-g7cc8g</i>)
pYY246	pXX206 <i>migS</i>
pYY249	pXX206 <i>migS-g10c</i>
pYY250	pXX206 <i>migS-c8g</i>
pYY252	pXX206 <i>migS-g7cc8g</i>
pYY260	pKD3 <i>migS</i> (46 bp DNA fragment including <i>migS</i>)
pYY265	pXX230 <i>migS</i>
pYY272	pKD3 <i>migS</i>

^aAll strains listed are derivatives of MC1061.

^bPlasmid harboring the split chromosomal segment.

References

Ben-Yehuda S, Rudner DZ, Losick R (2003) RacA, a bacterial protein that anchors chromosomes to the cell poles. *Science* 299: 532–536

ml), kanamycin (15 µg/ml), neomycin (7.5 µg/ml), spectinomycin (100 µg/ml), streptomycin (100 µg/ml), and tetracycline (1, 5, or 15 µg/ml). The generation time (doubling time) was determined by the turbidity of cultures. Genetic coordinates in minutes and bases were from the Profiling of *E. coli* Chromosome database (PEC: <http://www.shigen.nig.ac.jp/ecoli/pec/>).

The construction of chromosome deletion strains was carried out according to Datsenko and Wanner (2000). Nucleotide sequences of endpoints of the deletions are shown in Supplementary Table I. Each deletion was confirmed by PCR analysis. The DNA fragment including *migS* and *cat* was integrated into other chromosomal locations by the above method. The integrated fragment was amplified from pYY260 or pYY272 using primers with 40-nt extensions that are homologous to target regions. Then the *cat* gene was deleted by FLP recombinase, if necessary.

Construction of chromosomal split strains

We constructed chromosomal split mutations by interchromosomal recombination between truncated neomycin-resistant genes according to Itaya and Tanaka (1997). The [ne] and [et] cassettes were integrated into points of interest on the chromosome according to Datsenko and Wanner (2000). The insertions were confirmed by PCR. Sequences of all oligonucleotides used in the PCR are available upon request. The [ne] and [et] cassettes were integrated in the *E. coli* chromosome in the same direction. Low copy-number plasmids containing the [eo] cassette and the [te] cassette were constructed, like the mini-F plasmid pYY159 and *oriC* plasmid pYY166.

Time-lapse imaging

The structure of bacterial nucleoids was clearly visualized by Manson and Powelson (1956) under a phase contrast microscope. In general, a concentration of gelatin from Bovine Bone (Wako, Osaka, Japan) from 20 to 40% by weight in culture broth is used for mounting bacterial cells. Here we used 23% gelatin dissolved in M9 or L medium for *E. coli* and 26% for *B. subtilis*. Note that the concentration for the best results could only be determined experimentally. Living cells were mounted in 200 µl of melted gelatin medium. Living cells incubated at 25 or 30°C were observed in an inverted microscope Axiovert 200M (Zeiss, Germany) fully controlled under a PC by Axiovision software (Zeiss, Germany), and images were captured by an AxioCam CCD camera system. The images were improved in the nucleoid outline using the “equalization” treatment of Adobe Photoshop ver. 7 (Supplementary Figure 3).

FISH

FISH was carried out according to the procedures described previously (Niki and Hiraga, 1997). The FISH probe to detect the *oriC* segment of the *E. coli* chromosome was prepared as described previously (Niki *et al.*, 2000). The EcoRI–BamHI segment containing the *rep* and *bla* genes from mini-F plasmid pXX705 was used to detect *oriC* plasmids. The probe for the *cat* gene was amplified by PCR using pKD3 as a template. When cells were grown in M9 medium, almost all cells had one or two *oriC* foci (Supplementary Table III).

Supplementary data

Supplementary data are available at *The EMBO Journal* Online.

Acknowledgements

We thank Richard D’Ari for a critical reading of the manuscript. We are grateful to H Aiba, B Wanner, and M Itaya for providing plasmids and strains. This work was supported by Grant-in-Aid for Scientific Research (B), Grant-in-Aid for Scientific Research on Priority Areas (B) and (C) “Genome Biology”, the Advanced and Innovative Research Program in Life Sciences from the Ministry of Education, Culture, Sports, Science and Technology of Japan, and a grant of PREST, Japan Science and Technology Corporation to HN.

- Davis MA, Austin SJ (1988) Recognition of the P1 plasmid centromere analog involves binding of the ParB protein and is modified by a specific host factor. *EMBO J* **7**: 1881–1888
- Draper GC, Gober JW (2002) Bacterial chromosome segregation. *Annu Rev Microbiol* **56**: 567–597
- Edwards DH, Errington J (1997) The *Bacillus subtilis* DivIVA protein targets to the division septum and controls the site specificity of cell division. *Mol Microbiol* **24**: 905–915
- Funnell BE (1988) Participation of *Escherichia coli* integration host factor in the P1 plasmid partition system. *Proc Natl Acad Sci USA* **85**: 6657–6661
- Glaser P, Sharpe ME, Raether B, Perego M, Ohlsen K, Errington J (1997) Dynamic, mitotic-like behavior of a bacterial protein required for accurate chromosome partitioning. *Genes Dev* **11**: 1160–1168
- Gordon GS, Shivers RP, Wright A (2002) Polar localization of the *Escherichia coli* *oriC* region is independent of the site of replication initiation. *Mol Microbiol* **44**: 501–507
- Gordon GS, Sitnikov D, Webb CD, Teleman A, Straight A, Losick R, Murray AW, Wright A (1997) Chromosome and low copy plasmid segregation in *E. coli*: visual evidence for distinct mechanisms. *Cell* **90**: 1113–1121
- Gordon GS, Wright A (2000) DNA segregation in bacteria. *Annu Rev Microbiol* **54**: 681–708
- Hiraga S (2000) Dynamic localization of bacterial and plasmid chromosomes. *Annu Rev Genet* **34**: 21–59
- Hiraga S, Ichinose C, Niki H, Yamazoe M (1998) Cell cycle-dependent duplication and bidirectional migration of SeqA-associated DNA–protein complexes in *E. coli*. *Mol Cell* **1**: 381–387
- Itaya M, Tanaka T (1997) Experimental surgery to create subgenomes of *Bacillus subtilis* 168. *Proc Natl Acad Sci USA* **94**: 5378–5382
- Jacob F, Brenner S, Cuzin F (1963) On the regulation of DNA replication in bacteria. *Cold Spring Harbor Symp Quant Biol* **28**: 329–348
- Jensen RB, Shapiro L (1999) The *Caulobacter crescentus* *smc* gene is required for cell cycle progression and chromosome segregation. *Proc Natl Acad Sci USA* **96**: 10661–10666
- Lemon KP, Grossman AD (1998) Localization of bacterial DNA polymerase: evidence for a factory model of replication. *Science* **282**: 1516–1519
- Lemon KP, Grossman AD (2001) The extrusion-capture model for chromosome partitioning in bacteria. *Genes Dev* **15**: 2031–2041
- Lewis PJ, Errington J (1997) Direct evidence for active segregation of *oriC* regions of the *Bacillus subtilis* chromosome and colocalization with the Spo0J partitioning protein. *Mol Microbiol* **25**: 945–954
- Libante V, Thion L, Lane D (2001) Role of the ATP-binding site of SopA protein in partition of the F plasmid. *J Mol Biol* **314**: 387–399
- Manson DJ, Powelson DM (1956) Nuclear division as observed in living bacteria by a new technique. *J Bacteriol* **71**: 474–479
- Mori H, Mori Y, Ichinose C, Niki H, Ogura T, Kato A, Hiraga S (1989) Purification and characterization of SopA and SopB proteins essential for F plasmid partitioning. *J Biol Chem* **264**: 15535–15541
- Niki H, Hiraga S (1997) Subcellular distribution of actively partitioning F plasmid during the cell division cycle in *E. coli*. *Cell* **90**: 951–957
- Niki H, Hiraga S (1998) Polar localization of the replication origin and terminus in *Escherichia coli* nucleoids during chromosome partitioning. *Genes Dev* **12**: 1036–1045
- Niki H, Hiraga S (1999) Subcellular localization of plasmids containing the *oriC* region of the *Escherichia coli* chromosome, with or without the *sopABC* partitioning system. *Mol Microbiol* **34**: 498–503
- Niki H, Jaffe A, Imamura R, Ogura T, Hiraga S (1991) The new gene *mukB* codes for a 177 kd protein with coiled-coil domains involved in chromosome partitioning of *E. coli*. *EMBO J* **10**: 183–193
- Niki H, Yamaichi Y, Hiraga S (2000) Dynamic organization of chromosomal DNA in *Escherichia coli*. *Genes Dev* **14**: 212–223
- Ogura T, Hiraga S (1983) Partition mechanism of F plasmid: two plasmid gene-encoded products and a *cis*-acting region are involved in partition. *Cell* **32**: 351–360
- Ohsumi K, Yamazoe M, Hiraga S (2001) Different localization of SeqA-bound nascent DNA clusters and MukF–MukE–MukB complex in *Escherichia coli* cells. *Mol Microbiol* **40**: 835–845
- Sawitzke J, Austin S (2001) An analysis of the factory model for chromosome replication and segregation in bacteria. *Mol Microbiol* **40**: 786–794
- Sawitzke JA, Austin S (2000) Suppression of chromosome segregation defects of *Escherichia coli* *muk* mutants by mutations in topoisomerase I. *Proc Natl Acad Sci USA* **97**: 1671–1676
- Watanabe E, Wachi M, Yamasaki M, Nagai K (1992) ATPase activity of SopA, a protein essential for active partitioning of F plasmid. *Mol Gen Genet* **234**: 346–352
- Webb CD, Teleman A, Gordon S, Straight A, Belmont A, Lin DC-H, Grossman AD, Wright A, Losick R (1997) Bipolar localization of the replication origin regions of chromosomes in vegetative and sporulating cells of *B. subtilis*. *Cell* **88**: 667–674
- Weitao T, Nordstrom K, Dasgupta S (1999) Mutual suppression of *mukB* and *seqA* phenotypes might arise from their opposing influences on the *Escherichia coli* nucleoid structure. *Mol Microbiol* **34**: 157–168
- Wu LJ, Errington J (2002) A large dispersed chromosomal region required for chromosome segregation in sporulating cells of *Bacillus subtilis*. *EMBO J* **21**: 4001–4011
- Yamaichi Y, Niki H (2000) Active segregation by the *Bacillus subtilis* partitioning system in *Escherichia coli*. *Proc Natl Acad Sci USA* **97**: 14656–14661